IEEE Access
Multidisciplinary | Rapid Review | Open Access Journal

Received June 20, 2019, accepted July 1, 2019, date of publication July 5, 2019, date of current version July 25, 2019.

Digital Object Identifier 10.1109/ACCESS.2019.2927129

A New Theory for Locating Line Fault in Power System: Theoretical Part

XIPENG ZHANG, NENGLING TAI, (Member, IEEE), PAN WU, CHUNJU FAN, XIAODONG ZHENG, (Member, IEEE), AND WENTAO HUANG, (Member, IEEE)
Department of Electrical Engineering, Shanghai Jiao Tong University, Shanghai 200240, China

Corresponding author: Xiaodong Zheng (xiaodongzheng@sjtu.edu.cn)

This work was supported in part by the National Natural Science Foundation of China under Grant 51877135, in part by the National Key Research and Development Program of China under Grant 2016YFB0900601, in part by the Shanghai Rising-Star Program under Grant 18QA1402100, and in part by the Key Laboratory of Control of Power Transmission and Conversion (SJTU), Ministry of Education under Grant 2015AB04.

ABSTRACT This paper proposes a theory for locating line fault based on the basic principle of time reversal. The proof has five steps. First, the theoretical voltage and current at the ends of the line are calculated based on the transmission equation of the line in the additional network after line fault occurred. Second, the loss and lossless mirror line are established according to the parameters of the actual line. Third, the values of the implemented sources at the ends of the mirror line are calculated based on the conjugate complex of the theoretical values of voltage and current in the first step. Fourth, the RMS value of the fault current is calculated by assuming that fault occurs at every point of the mirror line. Finally, we should identify that there is only one peak value among all the RMS values and it exists at the actual fault location. In this paper, the fault location theory is proved with and without reflected waves by using the transmission equation of a single line. It is further proved in the mixed line that consists of two lines of different parameters considering the reflections.

INDEX TERMS Time reversal, mirror line, global peak value, mixed line.

I. INTRODUCTION

Line fault location technique is an eternal topic and research area of the power system. Many researchers and engineers are investigating and developing the method for line fault location [1], [2].

For the AC transmission lines, high-voltage and medium-voltage AC distribution lines, there are three fault location theories and methods which are the travelling-wave-based method, impedance method, and transients-analysis-based method [3]–[5]. For the low-voltage AC distribution network, its topologies are complicated with many branches. The locations and precision of measurements are not unified in practice so the feasibility and accuracy of fault location is low [6], [7].

The fault location methods in high voltage direct current system (HVDC) and voltage source converter based HVDC system (VSC-HVDC) are derived from the theories of the AC systems [8], [9]. The fault location in DC distribution network is in research stage because the practical projects and its topologies are in design and construction [10]–[12].

The associate editor coordinating the review of this manuscript and approving it for publication was Zhigang Liu.

The travelling-wave-based fault location method shows good performance in AC and DC systems. The key of this method is to extract the travelling wave front. Many digital signals processing technologies such as Hilbert-Huang and wavelet transform are in use [13], [14]. Based on the arrival time of travelling wave front, the fault location can be calculated by using one measurement or two measurements. The method using one measurement needs to detect the arrival time of the first and the second travelling wave front, while the two-measurements-based method detects the first travelling wave front at both the ends of the line. The calculation formula of this method is simple, but the method requires high performance hardware and travelling wave front is difficult to detect during high fault resistance [15]–[17].

The impedance method locates the fault in the overhead lines that ignore the capacitance. It uses the linear relationship between the measured impedance and the fault distance. However, the low precision of this method limits its application [4], [18].

The transients-analysis-based method is also a main investigative approach for line fault location [19]. One representative method locates the line fault by utilizing the properties that the voltage at the fault point is the lowest and in

phase with current. The line model and the calculation of the theoretical values of the transients are the basis of this method. For AC lines, the component of power frequency is selected for calculation based on the frequency-dependent line mode [20], [21]. For DC lines, it is difficult to select a component of a specific frequency from the measured distorted step signals for further calculation because the line faults generate a step signal that transmits along the lines. Some researchers use the Bergeron line model to analyze the transients in frequency domain. But the calculated transients are deviate from the actual signals as this line model differs greatly from the actual line. Therefore, the application of this method in DC lines needs improvement.

The theory of travelling-wave-based method has several advantages such as simple computation and robustness against different fault situations. The advantage of the transient-analysis-based method is low hardware requirement.

In order to combine the benefits of these two methods, the time-reversed-based method is created. The time reversal theory was first proposed for finding the ultrasound source in the ultrasonic fields. Then it is used for locating the location of lightning in the space. The correctness of the method is proved based on the time-reversed Maxwell's equations [22]–[25]. The application of locating lightning based on time reversal theory tells us that the source of field can be located through the initial incident waves generated by the source. Moreover, if the field contains the reflected waves or the waves come from other sources, the results would have large errors.

There are few essays for the fault location in power networks by using the time reversal theory. In [26], the fault is simulated in a constant-parameter line model in the AC distribution network. The fault location is then calculated by using one observer after the measured transient voltages are time reversed. The overhead line and the cable parameters are inferred from typical geometries of 230 kV lines and cable during the calculation in the time-reversed process. In [27], the fault is simulated in the frequency-independent line model in the multi-terminal VSC-HVDC system. The fault location is then calculated by using multiple observers after the measured currents of high frequency are time reversed. A lossless line is used when the fault currents of guessed fault locations are calculated. The method in [26] is developed as shown in [28]. Three types of back-propagation models are established for fault location by referring to [25]. The differences between these models are compared and the lossy back-propagation model is selected for fault location.

The theoretical parts in [26]–[28] are simply proved in the lossless line although the simulation case studies achieve good results in loss lines. Therefore, the method proposed in [26]–[28] are lack of a convincing theory.

In [29], the researchers defined a function that is a ratio of an ideal additional voltage in the actual line to a calculated guessed voltage in the time reversal process. The angle of the function will exceed a fixed range when the calculated guessed voltage is at the actual fault point. The proposed method is proved correct by using long-line equation in the line model of distributed parameters. However, this method has two defects. One is that the ideal additional voltage source is regarded as a step signal. The other is that it needs ultrahigh sampling frequency for calculating the angles of the defined function.

In this paper, the process of fault location theory is inherited from the method [25]–[28]. The theory proof in [26]–[28] are included in Section II-A in this paper. The theory of locating fault in line model of distribute parameters are firstly proved correct by using different mirror lines in this paper. In addition, the novel theory of locating fault in mixed line is proposed and proved correct. In the proof process, the form of the additional voltage source does not affect the fault location result. The skin effects of line parameters are also considered. These two advantages are exactly what the theory does not possess in [29]. The distinctive feature of the theory proof in this paper is based on the equations of the long-line equations which are the same to the proof process in [25]–[29].

II. LOCATING LINE FAULT WITHOUT CONSIDERING REFLECTED WAVE

In [25], the observers locating lightning are not affected by the reflected electromagnetic wave. In this section, the theory of fault location using time reversal is proposed without considering the reflected wave in the lines. The fault location considering reflected waves is further discussed in the following sections based on the proofs in this section.

In this paper, the proposed theory is proved in a single line in time domain and frequency domain. In practice, the fault point can be calculated by using transmission equation of positive-sequence, negative-sequence or zero-sequence line for AC systems. For DC systems, the fault location can be achieved in a single line of 1-mode or 0-mode parameters.

In this section, the fault location is calculated by using the currents at two-ends of the line.

A. LOSSLESS LINE

This subsection proves the theory of fault location in lossless line in time domain, and the steps of justification are introduced.

The additional network after fault occurrence is shown in Fig. 1(a). The total length of the line is l, and the distributed inductance and capacitance of the line are indicated as L and C, respectively. Suppose a fault occurred at l_1, the value of additional voltage source is u_F and the currents generated by this voltage source flows to the two ends of the line. Because the reflected currents are ignored, the magnitudes of generated currents are the same in two directions, which is indicated as i_F. Because the currents 'i_F' are the initial current forward travelling wave and the wave impedances of the lines in both sides of the additional vlotage source are equal, the currents 'i_F' in both directions in Fig. 1(a) are the same.

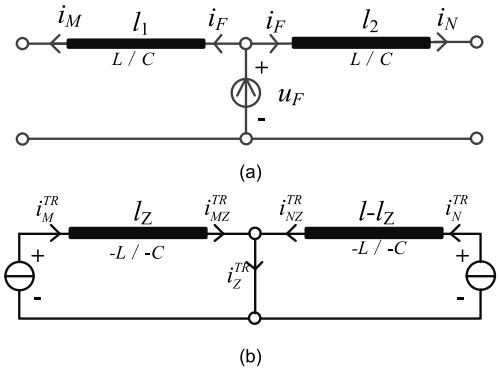

FIGURE 1. Justification for lossless line without reflected currents: (a) additional network after fault occurrence in time domain, (b) the fault current at the assumed fault point in mirror line in time domain.

The first step of justification is to calculate the theoretical value of the measured currents i_M and i_N. The values are calculated as follows:

$$i_M(t) = i_F(t - l_1/v)\, i_N(t) = i_F(t - l_2/v) \tag{1}$$

where, $v = 1/\sqrt{LC}$, which is the velocity of current wave.

The second step is time reversal, which is to reverse the measured signals in time axis. The theoretical values of measured signals are time-reversed in this proof. In practice, the period of measured signals (or theoretical values) is T so the currents in (1) is time-reversed and it is shown in (2).

$$\begin{cases} i_M^{TR}(t) = i_M(T - t) = i_F[T - (t - l_1/v)] \\ i_N^{TR}(t) = i_N(T - t) = i_F[T - (t - l_2/v)] \end{cases} \tag{2}$$

where, i_M^{TR} represents the time-reversed currents of $i_M(t)$.

As is shown in Fig.2, the time reversal of signal is to reverse the whole signal in time axis and the time-reversed signal should have numerical definitions in the scope of $[t_1, t_1 + T]$. Therefore, i_M^{TR} is expressed in (2), rather than $i_F[T - t - l_1/v]$.

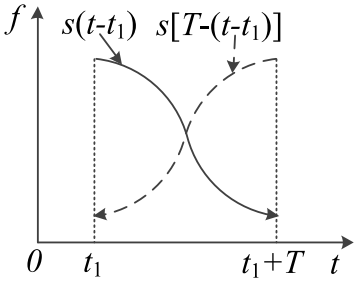

FIGURE 2. Schematic diagram of time reversal for signals.

The third step is to establish the mirror line of the actual line as is shown in Fig. 1(b), and the distributed inductance and capacitance are set as $-L$ and $-C$ respectively.

The fourth step is to implement the virtual sources at the terminals of the line. The sources are time-reversed currents in (2) in this procedure.

Finally, we can obtain a series of RMS values of fault currents by assuming a fault at every point of the mirror line and we should prove that the peak value of the RMS values occurs only at the place where the actual fault location is.

The fault current of assumed fault in Fig. 1(b) is shown in (3), which also does not consider the reflected currents.

$$\begin{aligned} i_Z^{TR}(t) &= i_{MZ}^{TR}(t) + i_{NZ}^{TR}(t) \\ &= i_M^{TR}(t - l_Z/v) + i_M^{TR}[t - (l - l_Z)/v] \\ &= i_F[T - (t - l_1/v) - l_Z/v] \\ &\quad + i_F[T - (t - l_2/v) - (l - l_Z)/v] \\ &= i_F[T - t + (l_1 - l_Z)/v] \\ &\quad + i_F[T - t + (l_Z - l_1)/v] \end{aligned} \tag{3}$$

Since the current (i_F) is defined within the time interval of $[0, T]$, the RMS value of i_Z^{TR} can be the peak value for $l_Z = l_1$ and the peak value is $2|i_F(T - t)|$.

The important and difficult parts of this theory are to establish a mirror line and the virtual sources in the mirror line as described in the previous third and fourth steps. The mirror line and virtual sources are built from the actual measurements and the parameters of the line. If we could prove only one peak value in the fifth (or last) step occurs at the actual location, no matter what forms the mirror line and virtual sources are, the steps of getting the two parameters can be regarded as correct, which enhancing the extensibility of the proposed method in this paper.

B. LOSS LINE

As is shown in Fig. 3(a), it is the additional network after line fault for loss line in frequency domain. Based on the transfer equation of line without considering the reflected currents, the theoretical value of current at end M can be expressed as follows:

$$I_M = (U_F/Z_C + I_F)\, e^{-\gamma l_1}/2 \tag{4}$$

where,

$$\begin{cases} Z_C = \sqrt{(R + jwL)/(G + jwC)} \\ \gamma = \sqrt{(R + jwL)(G + jwC)} = \alpha + j\beta \\ \alpha = \left\{\left[\left(R^2 + w^2L^2\right)\left(G^2 + w^2C^2\right)\right]^{1/2} \right. \\ \left. - w^2LC + RG\right\}^{1/2}/\sqrt{2} \\ \beta = \left\{\left[\left(R^2 + w^2L^2\right)\left(G^2 + w^2C^2\right)\right]^{1/2} \right. \\ \left. + w^2LC + RG\right\}^{1/2}/\sqrt{2} \end{cases} \tag{5}$$

$R/G/L/C$ are the distributed resistance, conductance, inductance and capacitance, respectively. w is the angular frequency. Z_C and γ are the wave impedance and transmission coefficient of the line, respectively.

The real signal that is time-reversed in time domain can get its conjugate signal in frequency domain. This conclusion is identified in appendix A. Therefore, the sources are the conjugate numbers of measured currents I_M and I_N as is shown in Fig. 3(b). The expression of the conjugated current (I^*_M) is $I_M^* = \left(U_F^*/Z_C^* + I_F^*\right) e^{-\gamma^* l_1}/2$.

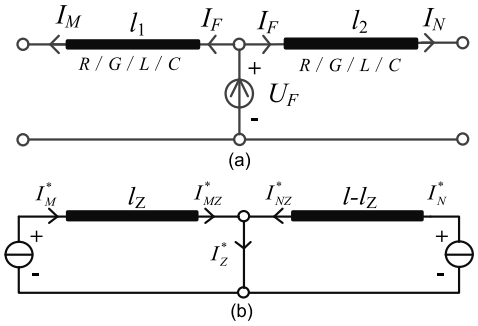

FIGURE 3. Justification for loss line without reflected currents: (a) additional network after fault occurrence in frequency domain, (b) the fault current at the assumed fault point in mirror line in frequency domain.

As is described in the last subsection, the next step of the proof is to establish the mirror line. We will introduce two types of mirror lines in the next subsections.

1) LOSSLESS MIRROR LINE

The distributed resistance, conductance, inductance and capacitance are set as 0, 0, $-L$ and $-C$ in Fig. 3(b), and it is called the lossless mirror line. The sources at the terminals of the mirror line are I_M^* and I_N^*. The fault current (I_{MZ}^*) generated from the current source at terminal M is a phase shift of I_M^* in frequency domain, which represents a time delay in time domain, and it can be calculated as:

$$\begin{aligned} I_{MZ}^* &= I_M^* e^{-j\beta_0 l_Z} = \left(U_F^*/Z_C^* + I_F^*\right) e^{-\gamma^* l_1} e^{-j\beta_0 l_Z}/2 \\ &= \left(U_F^*/Z_C^* + I_F^*\right) e^{-\alpha l_1} e^{-j(\beta_0 l_Z - \beta l_1)}/2 \end{aligned} \tag{6}$$

where, $\beta_0 = w\sqrt{LC}$.

The fault current (I_{NZ}^*) can also be calculated in the same way as I_{MZ}^*, which is shown in (7):

$$I_{NZ}^* = \left(U_F^*/Z_C^* + I_F^*\right) e^{-\alpha l_2} e^{-j[\beta_0(l-l_Z)-\beta l_2]}/2 \tag{7}$$

The fault current at the assumed fault location (l_Z) is the sum of the two currents in (6) and (7), and the modulus of fault current is:

$$\begin{aligned} \left|I_Z^*\right| &= \left|I_{MZ}^* + I_{NZ}^*\right| \\ &= \left|\left(U_F^*/Z_C^* + I_F^*\right)/2\right| \left|e^{-\alpha l_1} e^{-j(\beta_0 l_Z - \beta l_1)}\right. \\ &\quad \left. + e^{-\alpha l_2} e^{-j[\beta_0(l-l_Z)-\beta l_2]}\right| \\ &= \left|\left(U_F^*/Z_C^* + I_F^*\right)/2\right| \left[e^{-2\alpha l_1} + e^{-2\alpha l_2} + \right. \\ &\quad \left. 2e^{-\alpha l} \cos\left(2\beta_0 l_Z - \beta l_1 + \beta l_2 - \beta_0 l\right)\right]^{1/2} \end{aligned} \tag{8}$$

Formula (8) gets the peak value at $2\beta_0 l_Z - \beta l_1 + \beta l_2 - \beta_0 l = 2n\pi (n = 0, \pm 1, \pm 2 \cdots)$, and the calculated fault location is:

$$l_Z = \beta l_1/\beta_0 + (\beta_0 - \beta)\, l/\beta_0 + n\pi/\beta_0 \tag{9}$$

The phase coefficient β_0 of mirror line is determined subjectively so it can be changed to β by modifying the inductance and capacitance of the lossless mirror line. Therefore, formula (9) is simplified as $l_Z = l_1 + n\pi/\beta$. However, the results of fault location are not unique, which can be further processed in two ways.

The first way is to select a proper component whose phase coefficient is small enough to make $\pi/\beta > l$ as β varies with frequencies due to the skin effect. The purpose of this way is to make the distance between adjacent results larger than the total length of the line.

The other way is to use the measured signals in a frequency band to calculate the fault current in Fig. 3(b), and the fault current of assumed fault in a frequency band can be calculated as follow:

$$\begin{aligned} \left|\int_{f_L}^{f_H} I_Z^*(f)df\right| &= \left|\int_{f_L}^{f_H} \left[\left(U_F^*/Z_C^* + I_F^*\right)/2\right]\right. \\ &\quad \left.\left[e^{-\alpha l_1} e^{-j\beta(l_Z - l_1)} + e^{-\alpha l_2} e^{-j\beta(l_1 - l_Z)}\right] df\right| \end{aligned} \tag{10}$$

where, f_L is the lower limit of frequency, and f_H is the higher limit of frequency. Formula (10) is the definite integral of (8), and the phase coefficient β_0 is replaced with β in (10).

To transform (10) into discrete form, an inequality can be obtained, which is:

$$\begin{aligned} \max\left|\int_{f_L}^{f_H} I_Z^*(f)df\right| &\le \Delta f \max\left\{\left|I_Z^*(f_L)\right| + \left|I_Z^*(f_L + \Delta f)\right|\right. \\ &\quad \left. + \cdots + \left|I_Z^*(f_L + N\Delta f)\right| + \left|I_Z^*(f_H)\right|\right\} \end{aligned} \tag{11}$$

where, $f = (f_H - f_L)/N$.

Each of the functions ($\left|I_Z^*(f)\right|, f \in [f_L, f_H]$) in (9) achieves its peak at the same location, which is $l_Z = l_1$. Thus the inequality can be changed into equality at the actual fault location of l_Z. Because $l_Z = l_1 + n\pi/\beta (n \neq 0)$ is not continuous as n is integer, there are always some functions at the right side of (11) that cannot achieve the peak value at $l_Z \neq l_1$. In conclusion, the fault location result is unique.

The method that uses the measured currents based on lossless mirror line has been applied for locating fault in DC lines.

2) LOSS MIRROR LINE

The distributed resistance, conductance, inductance and capacitance is set as R, G, $-L$ and $-C$ in Fig. 3(b), and it is called the loss mirror line. We can obtain the fault current of assumed fault (I_{MZ}^*) in the loss mirror line, which is:

$$\begin{aligned} I_{MZ}^* &= I_M^* e^{-\gamma^* l_Z} = \left(U_F^*/Z_C^* + I_F^*\right) e^{-\gamma^* l_1} e^{-\gamma^* l_Z}/2 \\ &= \left(U_F^*/Z_C^* + I_F^*\right) e^{-\alpha(l_1 + l_Z)} e^{j\beta(l_1 + l_Z)}/2 \end{aligned} \tag{12}$$

The current I_{NZ}^* is also got the same way as (12) and the RMS value of fault current at l_Z is:

$$\begin{aligned} \left|I_Z^*\right| &= \left|I_{MZ}^* + I_{NZ}^*\right| \\ &= \left|\left(U_F^*/Z_C^* + I_F^*\right)/2\right| \left|e^{-\alpha(l_1 + l_Z)} e^{j\beta(l_1 + l_Z)}\right. \\ &\quad \left. + e^{-\alpha(l_2 + l - l_Z)} e^{j\beta(l_2 + l - l_Z)}\right| \end{aligned}$$

$$= \left|\left(U_F^*/Z_C^* + I_F^*\right)/2\right| \left[e^{-2\alpha(l_1+l_Z)} + e^{-2\alpha(l_2+l-l_Z)} + 2e^{-2\alpha l}\cos 2\beta\,(l_Z - l_2)\right]^{1/2} \quad (13)$$

A derivative for $\left|I_Z^*\right|^2$ is calculated for finding the global maximum of (13), which is:

$$d\left|I_Z^*\right|^2/dl_Z = \left|\left(U_F^*/Z_C^* + I_F^*\right)/2\right|^2 \left[-2\alpha e^{-2\alpha(l_1+l_Z)} + 2\alpha e^{-2\alpha(l_2+l-l_Z)} - 4\beta e^{-2\alpha l}\sin 2\beta\,(l_Z - l_2)\right] \quad (14)$$

Let $d\left|I_Z^*\right|^2/dl_Z = 0$ in (14), we can obtain the follow equation:

$$\underbrace{\alpha e^{-2\alpha(l_Z-l_2)} - \alpha e^{2\alpha(l_Z-l_2)}}_{f_1(l_Z)} = \underbrace{-2\beta\sin 2\beta\,(l_Z - l_2)}_{f_2(l_Z)} \quad (15)$$

Fig. 4(a) shows the graphs of two functions in the right and left side of (15). Because the value of α is smaller than that of β, formula (15) gets its peak value at least three locations according to the graph in Fig. 3(a). Therefore, the fault location result is not unique by calculating the global peak value of (13). In addition, if the value of α is closer to that of β, the wrong fault location result would be closer to l_2. So the method is not suitable for fault location.

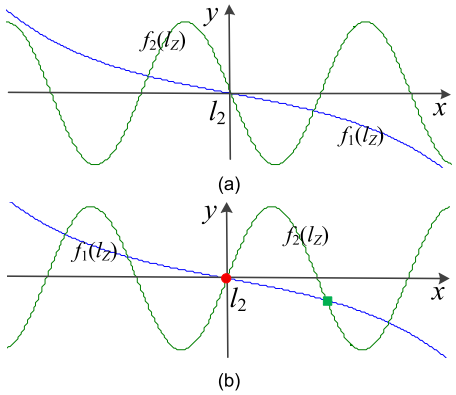

FIGURE 4. Graphic solution for transcendental equations: (a) the solution of (15), (b) the solution of (17).

In order to solve this problem, we can change formula (13) into (16) to calculate the fault current.

$$\left|I_Z^*\right| = \left|I_{MZ}^* - I_{NZ}^*\right| = \left|\left(U_F^*/Z_C^* + I_F^*\right)/2\right| \left[e^{-2\alpha(l_1+l_Z)} + e^{-2\alpha(l_2+l-l_Z)} - 2e^{-2\alpha l}\cos 2\beta\,(l_Z - l_2)\right]^{1/2} \quad (16)$$

Let $d\left|I_Z^*\right|^2/dl_Z = 0$ in (16), we can obtain the follow equation:

$$\underbrace{\alpha e^{-2\alpha(l_Z-l_2)} - \alpha e^{2\alpha(l_Z-l_2)}}_{f_1(l_Z)} = \underbrace{2\beta\sin 2\beta\,(l_Z - l_2)}_{f_2(l_Z)} \quad (17)$$

Fig. 4(b) shows the graphs of two functions in the right and left side of (17). As is seen from the graphs, formula (16) gets the minimum value when $l_Z = l_2$. However, formula (16) has multiple same minimum values as is shown in Fig. 4(b), we can solve this problem through three ways.

The first way is to find a proper value of β to make $l < \pi/(2\beta)$ because the distance between the red point (actual fault location) and the green point (redundant fault location) in Fig. 4(b) is always large than $\pi/2$.

The second way is to find proper values of α and β to make $f_1(l_Z)$ and $f_2(l_Z)$ only intersect at l_2 in Fig. 3(b).

The last way is to use signals of frequency band to locate the fault location as is introduced in the last subsection.

3) BRIEF SUMMARY

The line fault can be located only through measured currents at the ends of the line without considering reflected current waves. It should be pointed out that the fault current of assumed fault in mirror line is calculated without reflections. Besides, we can also set the fault resistance of assumed fault to be the value of the wave impedance of the mirror line. The reflections will not exist in this situation.

The method based on the lossless mirror line can be easily applied into the fault location in both time and frequency domain, while the method based on the loss mirror line can be used in the frequency domain.

Because the measured transients at the ends of the DC lines are distorted step signals, it is not accurate to represent the transients in frequency domain. Therefore, the method based on the lossless mirror line is applied into the fault location in the DC lines. The loss mirror line-based method is applied into the fault location in the AC lines.

III. LOCATING LINE FAULT WITH CONSIDERING REFLECTED WAVE

The lightning fault location in [25] and the line fault location in section II indicate that the electromagnetic sources can be located without reflections. However, the voltage and current waves are reflected between the fault point and the line terminals. In order to eliminate the effects of the reflections, the voltage and current forward travelling wave are used for locating fault with reflections based on the experience in the previous introduction.

In this section, the fault location is calculated by using both the voltages and currents at two-ends of the line.

A. LOSS LINE

As is shown in Fig. 5(a), it is the fault additional network after line fault occurrence. Z_M and Z_N are the equivalent impedances of the systems at the ends of the line. The theoretical values of U_M and I_M are calculated based on two conditions. One is the line-to-ground voltage (U_F) at the fault point, the other is that the equivalent impedance Z_M equals to the ratio of U_M and I_M at the terminal M. By combining the

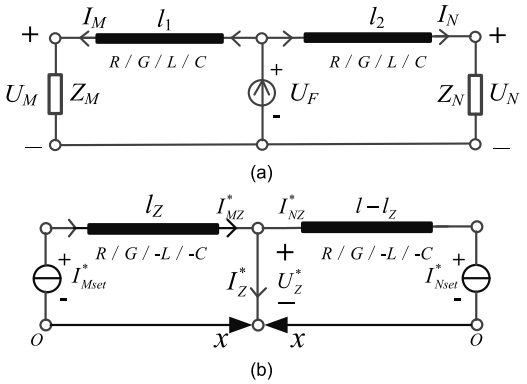

FIGURE 5. Justification for loss line with reflected currents: (a) additional network after fault occurrence, (b) the fault current at the assumed fault point in mirror line in frequency domain.

long-line equation, we can obtain the following equation:

$$\begin{cases} U_F = U_+ + U_- \\ U_M = U_+ e^{-\gamma l_1} + U_- e^{\gamma l_1} \\ I_M = I_+ e^{-\gamma l_1} + I_- e^{\gamma l_1} \\ Z_M = U_M / I_M \end{cases} \tag{18}$$

By solving (18), the voltage and current forward travelling wave (U_+/I_+) and the voltage and current backward travelling wave (U_-/I_-) can be obtained by using $U_F/Z_M/Z_C$, as is shown in (19):

$$\begin{cases} U_+ = U_F/\left(1+\Gamma_M e^{-2\gamma l_1}\right) & I_+ = U_+/Z_C \\ U_- = U_F - U_F/\left(1+\Gamma_M e^{-2\gamma l_1}\right) & I_- = -U_-/Z_C \\ \Gamma_M = (Z_M - Z_C)/(Z_C + Z_M) \end{cases} \tag{19}$$

where, Γ_M is the reflection coefficient, Z_C and γ are introduced in (5).

As is shown in Fig. 5(b), the mirror loss line is established and the distributed parameters are displayed in the figure. The wave impedance and transmission coefficient of the mirror loss line are Z^*_C and γ^* respectively.

After the loss mirror line was established, the sources in the mirror line need to be set. Let the current sources at the terminals of the line be I^*_{Mset} and I^*_{Nse}. In addition, suppose that a metallic fault occurred at l_Z of the mirror line. Based on two known quantities, which are the pre-set current source at terminal M and the voltage (equals to zero) at l_Z., formula (20) can be obtained the same as (18).

$$\begin{cases} I^*_{Mset} = I_+ + I_- \\ I^*_{MZ} = I_+ e^{-\gamma^* l_Z} + I_- e^{\gamma^* l_Z} \\ U^*_Z = Z_C I_+ e^{-\gamma^* l_Z} - Z_C I_- e^{\gamma^* l_Z} = 0 \end{cases} \tag{20}$$

The fault current of assumed fault (I^*_{MZ}) can be calculated from (20), which is:

$$I^*_{MZ} = \frac{2I^*_{Mset} e^{-\gamma^* l_z}}{1 + e^{-2\gamma^* l_z}} \tag{21}$$

It should be pointed out that it is for calculation convenience to set the metallic fault in the mirror line. It does not represent the actual fault resistance.

In practice, U_M and I_M are measured signals. In addition, Z_M and Z_C are known. Therefore, I^*_{Mset} can be defined as:

$$I^*_{Mset} = \frac{1}{U^*_M/Z^*_C + I^*_M} \frac{1 + e^{-2\gamma^* l_Z}}{1 + \Gamma^*_M e^{-2\gamma^* l_Z}} \tag{22}$$

To substitute (18) and (19) into (22), the theoretical value of I^*_{Mset} is $\frac{Z^*_C\left(1+\Gamma^*_M e^{-2\gamma^* l_1}\right)}{2U^*_F e^{-\gamma^* l_1}} \frac{1+e^{-2\gamma^* l_Z}}{1+\Gamma^*_M e^{-2\gamma^* l_Z}}$.

Then, to substitute (22) into (21), we can obtain (23):

$$I^*_{MZ} = \frac{Z^*_C}{U^*_F} \frac{e^{-\gamma^* l_Z}}{e^{-\gamma^* l_1}} \frac{1 + \Gamma^*_M e^{-2\gamma^* l_1}}{1 + \Gamma^*_M e^{-2\gamma^* l_Z}} \tag{23}$$

Similarly, the current I^*_{NZ} is also as:

$$I^*_{NZ} = \frac{Z^*_C}{U^*_F} \frac{e^{-\gamma^*(l-l_Z)}}{e^{-\gamma^* l_2}} \frac{1 + \Gamma^*_N e^{-2\gamma^* l_2}}{1 + \Gamma^*_N e^{-2\gamma^*(l-l_Z)}} \tag{24}$$

where, $\Gamma_N = (Z_N - Z_C)/(Z_C + Z_N)$ which is a reflection coefficient.

In order to get the fault location, let:

$$\begin{aligned} \left|I^*_Z\right| &= \left|I^*_{MZ} - I^*_{NZ}\right| \\ &= \left|\frac{Z^*_C}{U^*_F}\right| \left| \frac{e^{-\gamma^* l_Z}}{e^{-\gamma^* l_1}} \frac{1 + \Gamma^*_M e^{-2\gamma^* l_1}}{1 + \Gamma^*_M e^{-2\gamma^* l_Z}} \right. \\ &\quad \left. - \frac{e^{-\gamma^*(l-l_Z)}}{e^{-\gamma^* l_2}} \frac{1 + \Gamma^*_N e^{-2\gamma^* l_2}}{1 + \Gamma^*_N e^{-2\gamma^*(l-l_Z)}} \right| \end{aligned} \tag{25}$$

Formula (25) gets the global minimum at $l_Z = l_1$, and the minimum value is 0. In order to identify that the location result is unique, let (25) equal to zero and then we can obtain:

$$\frac{e^{\gamma^* l_1} + \Gamma^*_M e^{-\gamma^* l_1}}{e^{\gamma^* l_Z} + \Gamma^*_M e^{-\gamma^* l_Z}} = \frac{e^{\gamma^* l_2} + \Gamma^*_N e^{-\gamma^* l_2}}{e^{\gamma^*(l-l_Z)} + \Gamma^*_N e^{-\gamma^*(l-l_Z)}} \tag{26}$$

After the simplification of (26), $e^{2\gamma^*(l_Z - l_1)} = 1$ which is a monotone function. As a results, the fault location result is unique.

B. IMPEDANCE LINE

In the distribution network of low rated voltage, the conductance and capacitance of the line can be neglected as the line is short.

As is shown in Fig. 6(a), the measured voltage at end M is

$$U_M = U_F Z_M / (Z_M + l_1 Z) \tag{27}$$

where, $Z = R + jwL$, which is a per unit impedance.

As is shown in Fig. 6(b), the per unit resistance and conductance of the loss mirror line is R/-L. As represented in the previous sections, the sources in the loss mirror line should be established. In this situation, the voltage source at end M is set as $U^*_{Mset} = U^*_M/Z^*_M$.

Then, the fault current of assumed fault (I^*_{MZ}) is

$$I^*_{MZ} = \frac{U^*_F}{\left(Z^*_M + l_1 Z^*\right)\left(Z^*_N + l_Z Z^*\right)} \tag{28}$$

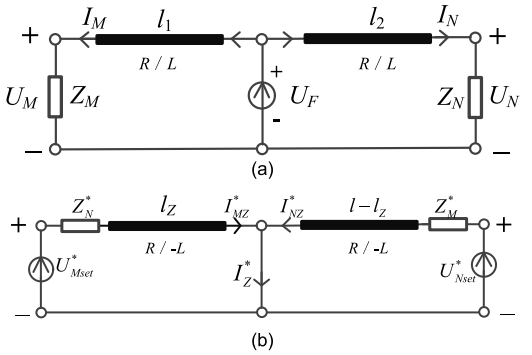

FIGURE 6. Justification for impedance line (a) additional network after fault occurrence, (b) the fault current at the assumed fault point in mirror line.

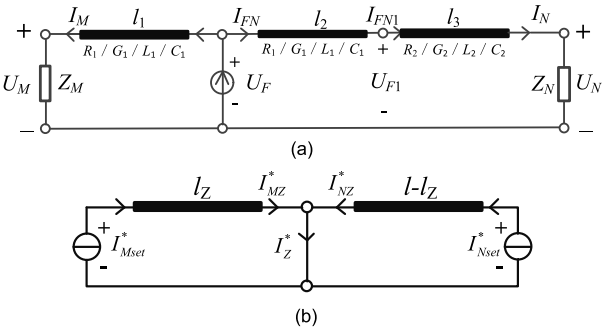

FIGURE 7. Justification of fault location for mixed line (a) additional network after fault occurrence, (b) the fault current at the assumed fault point in mirror line.

The other fault current I_{NZ}^* is calculated in the same way.

$$I_{NZ}^* = \frac{U_F^*}{\left(Z_N^* + l_2 Z^*\right)\left[Z_M^* + (l - l_Z)\, Z^*\right]} \tag{29}$$

Finally, the modulus of I_Z^* is calculated as:

$$\begin{aligned} \left|I_Z^*\right| &= \left|I_{MZ}^* - I_{NZ}^*\right| \\ &= \left|U_F^*\right| \left| \frac{1}{\left(Z_M^* + l_1 Z^*\right)\left(Z_N^* + l_Z Z^*\right)} \right. \\ &\quad \left. - \frac{1}{\left(Z_N^* + l_2 Z^*\right)\left[Z_M^* + (l - l_Z)\, Z^*\right]} \right| \end{aligned} \tag{30}$$

$\left|I_Z^*\right|$ can achieve its global minimum only as $l_Z = l_1$, and the fault location can be located.

In this subsection, the proposed theory for fault location in short lines are introduced, and it guarantees the expandability and integrity of the theory.

IV. LOCATING FAULT IN MIXED LINE

The actual line that consists of lines of different parameters is called the mixed line. In this section, the fault location theory for mixed line of two parameters is proved.

In this section, the fault location is calculated by using both the voltages and currents at two-ends of the line.

As is shown in Fig. 7(a), two lines of different parameters are connected, the total length of the first line is $l_1 + l_2$, and its distributed parameters are $R_1/G_1/L_1/C_1$; the total length of the second line is l_3 whose distributed parameters $R_2/G_2/L_2/C_2$.

Suppose that a fault occurred at l_1, the theoretical values of measured voltage and current at end M are the same as are shown in (18) and (19). The theoretical values of the measurements at end N is complex and is to be calculated as follows.

The electrical equations at both ends of the line (l_2 and l_3) are obtained according to the long-line equation. The electrical equations are shown in (31) and (32) respectively.

$$\begin{cases} U_F = U_{1+}^N + U_{1-}^N \\ I_{FN} = I_{1+}^N + I_{1-}^N \end{cases} \quad \begin{cases} U_{F1} = U_{1+}^N e^{-\gamma_1 l_2} + U_{1-}^N e^{\gamma_1 l_2} \\ I_{FN1} = I_{1+}^N e^{-\gamma_1 l_2} + I_{1-}^N e^{\gamma_1 l_2} \end{cases} \tag{31}$$

$$\begin{cases} U_{F1} = U_{2+}^N + U_{2-}^N \\ I_{FN1} = I_{2+}^N + I_{2-}^N \end{cases} \quad \begin{cases} U_N = U_{2+}^N e^{-\gamma_2 l_3} + U_{2-}^N e^{\gamma_2 l_3} \\ I_N = I_{2+}^N e^{-\gamma_2 l_3} + I_{2-}^N e^{\gamma_2 l_3} \end{cases} \tag{32}$$

where, (i =1,2)

$$\begin{cases} \gamma_i = \sqrt{(R_i + jwL_i)\,(G_i + jwC_i)} = \alpha_i + j\beta_i \\ Z_{Ci} = \sqrt{(R_i + jwL_i)/(G_i + jwC_i)} \\ U_{i+}^N / I_{i+}^N = Z_{Ci}\; U_{i-}^N / I_{i-}^N = -Z_{Ci} U_N / I_N = Z_N \end{cases} \tag{33}$$

Because the theoretical values of the measurements at end N are complicated, it is impossible to establish a mirror source as (22) for further process. Therefore, a novel and practical theory for fault location of mixed line is proposed in this paper and it is proved and introduced into next steps.

$$\begin{aligned} &I_{N\text{set}} \\ &= \left[\left(U_N \Big/ \underbrace{Z_{C2}}_{local} + I_N \right) \left(\underbrace{Z_{C2}}_{local} + \underbrace{Z_{C1}}_{opposite} \right) \Big/ 2 \right. \\ &\quad \left. + \left(U_N \Big/ \underbrace{Z_{C2}}_{local} - I_N \right) \right. \\ &\quad \left. \left(\underbrace{Z_{C2}}_{local} - \underbrace{Z_{C1}}_{opposite} \right) \Big/ 2 \right] \Big/ \left(2\, \underbrace{Z_{C1}}_{opposite} \right) \\ &= \left[I_{2+}^N e^{-\gamma_2 l_3} (Z_{C2} + Z_{C1}) - I_{2-}^N e^{-\gamma_2 l_3} (Z_{C2} - Z_{C1}) \right] \Big/ 2Z_{C1} \\ &= e^{-\gamma_2 l_3} \left(I_{2+}^N Z_{C2} - I_{2-}^N Z_{C2} + I_{2+}^N Z_{C1} + I_{2-}^N Z_{C1} \right) \Big/ 2Z_{C1} \\ &= e^{-\gamma_2 l_3} \left[U_{2+}^N + U_{2-}^N + Z_{C1} \left(I_{2+}^N + I_{2-}^N \right) \right] \Big/ 2Z_{C1} \\ &= e^{-\gamma_2 l_3} \left(U_{F1} + Z_{C1} I_{FN1} \right) \Big/ 2Z_{C1} \\ &= I_{1+}^N e^{-\gamma_1 l_2} e^{-\gamma_2 l_3} \end{aligned} \tag{34}$$

Step1: based on the known parameters of the line and measurements (U_N/I_N), the current forward travelling wave generated by fault occurrence is obtained as shown in (34).

where, '*local*' represents the wave impedance of the line that is directly connected to end N, '*opposite*' represents the wave impedance of the line that the opposite end M directly connected to. I_{1+}^{N} in (35) is calculated by (32) and (33), and its solution procedure is in appendix B.

$$I_{1+}^{N} = \frac{U_F}{Z_{C1}\left(1 + \frac{\Gamma+\Gamma_N e^{-2\gamma_2 l_3}}{1+\Gamma\Gamma_N e^{-2\gamma_2 l_3}} en^{-2\gamma_1 l_2}\right)} \tag{35}$$

where, $\Gamma = (Z_{C2} - Z_{C1})/(Z_{C1} + Z_{C2})$, which is the reflection coefficient at the connection of two different lines. $\Gamma_N = (Z_N - Z_{C2})/(Z_N + Z_{C2})$ is also a reflection coefficient.

Step2: in practice, the measurements at the two ends of the line should perform the same algorithm so that the measurements will be handled symmetrically. The current forward travelling wave at end M is obtained as:

$$\begin{aligned} I_{Mset} &= \left[\left(U_M/Z_{C1} + I_M\right)(Z_{C1} + Z_{C2})/2 \right. \\ &\quad \left. +\left(U_M/Z_{C1} - I_M\right)(Z_{C1} - Z_{C2})/2\right]/(2Z_{C2}) \\ &= \left[I_{1+}^{M} e^{-\gamma_1 l_1}(Z_{C1}+Z_{C2}) - I_{1-}^{M} e^{\gamma_1 l_1}(Z_{C1}-Z_{C2})\right]/(2Z_{C2}) \\ &= \left[I_{1+}^{M} e^{-\gamma_1 l_1}(Z_{C1} + Z_{C2}) + I_{1-}^{M} e^{-\gamma_1 l_1} \right. \\ &\quad \left. \Gamma_M (Z_{C1} - Z_{C2})\right]/(2Z_{C2}) \\ &= I_{1+}^{M} e^{-\gamma_1 l_1}[(Z_{C1} + Z_{C2}) + \Gamma_M (Z_{C1} - Z_{C2})]/(2Z_{C2}) \end{aligned} \tag{36}$$

where, $I_{1+}^{M} = U_F/\left[Z_{C1}\left(1 + \Gamma_M e^{-2\gamma_1 l_1}\right)\right]$.

Step3: as is shown in Fig. 7(b), the fault current of assumed fault is calculated in the lossless mirror line ignoring the reflections.

Let the complex number in (37) be the polar form as:

$$\begin{aligned} U_F^*/Z_{C1}^* &= Ae^{j\theta_0} \\ \frac{\left[\left(Z_{C1}^* + Z_{C2}^*\right) + \Gamma_M^*\left(Z_{C1}^* - Z_{C2}^*\right)\right]}{2\left(1 + \Gamma_M^* e^{-2\gamma_1^* l_1}\right) Z_{C2}^*} &= Be^{j\theta_1} \\ 1\Big/\left(1 + \frac{\Gamma^* + \Gamma_N^* e^{-2\gamma_2^* l_3}}{1 + \Gamma^*\Gamma_N^* e^{-2\gamma_2^* l_3}} e^{-2\gamma_1^* l_2}\right) &= Ce^{j\theta_2} \end{aligned} \tag{37}$$

where, A, B and C are the real number.

If $0 \le l_Z \le l_1 + l_2$, the fault current of assumed fault in Fig. 7(b) is calculated, which is expressed in (38) by substituting (37) into (34) and (36).

$$\begin{aligned} I_Z^* &= I_{MZ}^* + I_{NZ}^* \\ &= I_{Mset}^* e^{-j\beta_1 l_Z} + I_{Nset}^* e^{-j\beta_2 l_3 - j\beta_1(l_1+l_2-l_Z)} \\ &= ABe^{-\alpha_1 l_1} e^{-j[\beta_1(l_Z - l_1) - \theta_1 - \theta_0]} \\ &\quad + ACe^{-\alpha_2 l_3 - \alpha_1 l_2} e^{-j[\beta_1(l_1 - l_Z) - \theta_0 - \theta_2]} \end{aligned} \tag{38}$$

If $l_1 + l_2 < l_Z \le l_1 + l_2 + l_3$, the current is

$$\begin{aligned} I_Z^* &= I_{MZ}^* + I_{NZ}^* \\ &= I_{Mset}^* e^{-j\beta_1(l_1+l_2) - j\beta_2(l_Z - l_1 - l_2)} + I_{Nset}^* e^{-j\beta_2(l_1+l_2+l_3-l_Z)} \\ &= ABe^{-\alpha_1 l_1} e^{-j\beta_1 l_2 - j\beta_2(l_Z - l_1 - l_2) + j(\theta_0+\theta_1)} \\ &\quad + ACe^{-\alpha_2 l_3 - \alpha_1 l_2} e^{j\beta_1 l_2 + j\beta_2(l_Z - l_1 - l_2) + j(\theta_0+\theta_2)} \end{aligned} \tag{39}$$

Step4: calculate the modulus of (38) and (39), and select the peak value to find the fault location. The fault location is obtained the same as (9).

$$l_{fault} = \begin{cases} l_1 + (\theta_1 - \theta_2)/2\beta_1 + n\pi/\beta_1 \\ (0 \le l_Z \le l_1 + l_2) \\ l_1 + l_2 - \beta_1 l_2/\beta_2 + (\theta_1 - \theta_2)/2\beta_2 + n\pi/\beta_2 \\ (l_1 + l_2 < l_Z \le l_1 + l_2 + l_3) \end{cases} \tag{40}$$

The fault location results in (40) are not the actual location. The errors have two parts. The first parts are $(\theta_1 - \theta_2)/2\beta_1$ and $(\theta_1 - \theta_2)/2\beta_2$ which are caused by the angle of complex number in (37). The second parts are and $n\pi/\beta_1$ and $n\pi/\beta_2$ which are called the periodic multiple errors.

According to the previous justification, the periodic multiple errors can be eliminated by using measured signals in a frequency band to calculate the fault location. However, the errors ($(\theta_1 - \theta_2)/2\beta_1$ and $(\theta_1 - \theta_2)/2\beta_2$) cannot be eliminated by using signals in a frequency band since θ_1 and θ_2 change with the fault locations. Therefore, the errors in (40) cannot be eliminated by using signals in a frequency band.

In order to eliminate the errors ($(\theta_1$-$\theta_2)/2\beta_1$ and $(\theta_1$-$\theta_2)/2\beta_2$) in (40), we can calculate the theoretical values of the errors in advance. Because the errors are determined by the impedances of the lines and the reflection coefficients as are shown in (37), the errors can be pre-calculated as is shown in '*error*' in (41), as shown at the top of the next page. Function $f(l_Z)$ represents the theoretical fault location result by using method III. Let $y = |f(l_Z)$-$l_{fault}|$. Calculate the minimum value of y, and the corresponding value of l_Z is the fault location result.

In order to eliminate the periodic multiple errors, the adjacent results (π/β_1 and π/β_2) can be moved out of the correct interval since the fault location results are between $\min\{f(l_Z)\}$ and $\max\{f(l_Z)\}$. Therefore, the values of β_1 and β_2 at a proper frequency can be selected for calculation as long as these two values can satisfy the inequality as is shown in (42).

$$\begin{aligned} &[\![\pi/\beta_1 > \max\{f(l_z), l_Z \in [0, l_1 + l_2]\}]\!] \text{ and} \\ &[\![\pi/\beta_2 > \max\{f(l_z), l_Z \in (l_1 + l_2, l_1 + l_2 + l_3]\} \\ &\pi/\beta_2 < \min\{f(l_Z), l_Z \in (l_1 + l_2, l_1 + l_2 + l_3]\}]\!] \end{aligned} \tag{42}$$

After $(\theta_1$-$\theta_2)/2\beta_1$, $(\theta_1$-$\theta_2)/2\beta_2$ and periodic multiple errors are eliminated, the fault location results in (40) will have only two. In addition, since $l_1 + l_2$-$\beta_1 l_2/\beta_2$ is not between $l_1 + l_2$ and $l_1 + l_2 + l_3$, this fault location result can be eliminated again. Therefore, the final result has only one when the fault is located in a proper frequency domain.

V. CONCLUSION

This paper proposes a time-reversal-based fault location theory with two measurements. No matter how the parameters

$$
\begin{aligned}
&f\left(l_Z\right)\\
&= l_Z + error\\
&= l_Z + \begin{cases}
\left\{\arg\left[\dfrac{\left[\left(Z_{C1}^{*}+Z_{C2}^{*}\right)+\Gamma_M^{*}\left(Z_{C1}^{*}-Z_{C2}^{*}\right)\right]}{2\left(1+\Gamma_M^{*}e^{-2\gamma_1^{*}l_Z}\right)Z_{C2}^{*}}\right]-\arg\left[1\Big/\left(1+\dfrac{\Gamma^{*}+\Gamma_N^{*}e^{-2\gamma_2^{*}l_3}}{1+\Gamma^{*}\Gamma_N^{*}e^{-2\gamma_2^{*}l_3}}e^{-2\gamma_1^{*}(l_1+l_2-l_Z)}\right)\right]\right\}\Big/(2\beta_1)\\
(0\le l_Z<l_1+l_2)\\
\left\{\arg\left[\dfrac{\left[\left(Z_{C1}^{*}+Z_{C2}^{*}\right)+\Gamma_M^{*}\left(Z_{C1}^{*}-Z_{C2}^{*}\right)\right]}{1+\Gamma_M^{*}e^{-2\gamma_1^{*}l_Z}}\right]-\arg\left[\dfrac{\left[\left(Z_{C1}^{*}+Z_{C2}^{*}\right)+\Gamma_M^{*}\left(Z_{C2}^{*}-Z_{C1}^{*}\right)\right]}{1+\Gamma_N^{*}e^{-2\gamma_1^{*}(l_1+l_2+l_3-l_Z)}}\right]\right\}\Big/(\beta_1+\beta_2)\\
(l_Z=l_1+l_2)\\
\left\{\arg\left[1\Big/\left(1+\dfrac{-\Gamma^{*}+\Gamma_M^{*}e^{-2\gamma_1^{*}(l_1+l_2)}}{1-\Gamma^{*}\Gamma_M^{*}e^{-2\gamma_1^{*}(l_1+l_2)}}e^{-2\gamma_2^{*}(l_Z-l_1-l_2)}\right)\right]-\arg\left[\dfrac{\left[\left(Z_{C1}^{*}+Z_{C2}^{*}\right)+\Gamma_N^{*}\left(Z_{C2}^{*}-Z_{C1}^{*}\right)\right]}{2\left(1+\Gamma_N^{*}e^{-2\gamma_2^{*}(l_1+l_2+l_3-l_Z)}\right)Z_{C1}^{*}}\right]\right\}\Big/(2\beta_2)\\
(l_1+l_2<l_Z\le l_1+l_2+l_3)
\end{cases}
\end{aligned}
\tag{41}
$$

of the mirror line are set, the proposed theory is effective, as long as the extrema of the RMS values of fault currents of assumed faults is proved to be only occurring at the actual fault location. The fault resistances and fault types according to the proposed justification do not affect the calculated result of fault location.

APPENDIX

A. JUSTIFICATION PROCESS

The Fourier transform is as follows: A.1

$$I\left(w\right)=\int_{-\infty}^{\infty}i\left(t\right)e^{-jwt}dt \tag{A.1}$$

To transform (A1) into its conjugate format, that is:

$$I^{*}\left(w\right)=\left[\int_{-\infty}^{\infty}i\left(t\right)e^{-jwt}dt\right]^{*}=\int_{-\infty}^{\infty}i^{*}\left(t\right)e^{jwt}dt \tag{A.2}$$

Because $i(t)$ is a real function, $i^{*}(t)$ can be replaced by $i(t)$ in (A.2). Then, the variable t is replaced by $-t$ in (A.2), and we can get (A.3).

$$I^{*}\left(w\right)=\int_{-\infty}^{\infty}i\left(t\right)e^{jwt}dt\overset{t\mapsto-t}{\longrightarrow}\int_{-\infty}^{\infty}i\left(-t\right)e^{-jwt}d\left(-t\right) \tag{A.3}$$

We can know that $\int_{-\infty}^{\infty}i\left(-t\right)e^{-jwt}d\left(-t\right)$ is the Fourier transform of $i(–t)$. In conclusion, the real function is time revered means that it can be conjugated in frequency domain.

B. DERIVATION PROCESS

Because $U_N/I_N = Z_N$, and by combining (32), we can get that:

$$\frac{U_{2+}^{N}e^{-\gamma_2 l_3}+U_{2-}^{N}e^{\gamma_2 l_3}}{I_{2+}^{N}e^{-\gamma_2 l_3}+I_{2-}^{N}e^{\gamma_2 l_3}}=Z_N \tag{A.4}$$

To replace I_{2+}^{N} and I_{2-}^{N} with U_{2+}^{N} and U_{2-}^{N} respectively, then (A.5) can be achieved.

$$U_{2+}^{N}e^{-\gamma_2 l_3}+U_{2-}^{N}e^{\gamma_2 l_3}=\frac{Z_N}{Z_{C2}}\left(U_{2+}^{N}e^{-\gamma_2 l_3}-U_{2-}^{N}e^{\gamma_2 l_3}\right) \tag{A.5}$$

Because the voltage and current remain unchanged at l_2, according to (31) and (32), we can get that:

$$\begin{cases}U_{F1}=U_{1+}^{N}e^{-\gamma_1 l_2}+U_{1-}^{N}e^{\gamma_1 l_2}=U_{2+}^{N}+U_{2-}^{N}\\ I_{FN1}=I_{1+}^{N}e^{-\gamma_1 l_2}+I_{1-}^{N}e^{\gamma_1 l_2}=I_{2+}^{N}+I_{2-}^{N}\end{cases} \tag{A.6}$$

To replace the $I_{1+}^{N}/I_{1-}^{N}/I_{2+}^{N}/I_{2-}^{N}$ with $U_{1+}^{N}/U_{1-}^{N}/U_{2+}^{N}/U_{2-}^{N}$ respectively, (A.7) can be achieved.

$$\begin{cases}2U_{2+}^{N}=U_{1+}^{N}e^{-\gamma_1 l_2}\left(1+Z_{C2}/Z_{C1}\right)\\ +U_{1-}^{N}e^{\gamma_1 l_2}\left(1-Z_{C2}/Z_{C1}\right)\\ 2U_{2-}^{N}=U_{1+}^{N}e^{-\gamma_1 l_2}\left(1-Z_{C2}/Z_{C1}\right)\\ +U_{1-}^{N}e^{\gamma_1 l_2}\left(1+Z_{C2}/Z_{C1}\right)\end{cases} \tag{A.7}$$

Finally, to combine (A.5) and (A.7), and based on $U_F = U_{1+}^{N}+U_{1-}^{N}$, formula (35) is obtained.

REFERENCES

[1] K. Chen, C. Huang, and J. He, "Fault detection, classification and location for transmission lines and distribution systems: A review on the methods," *High Voltage*, vol. 1, no. 1, pp. 25–33, Apr. 2016.

[2] M. Dragomir, A. Miron, M. Istrate, and A. Dragomir, "A review of impedance-based fault location approaches for transmission lines," in *Proc. Int. Conf. Expo. Elect. Power Eng. (EPE)*, Iasi, Romania, 2014, pp. 1021–1024.

[3] T. Hinge and S. Dambhare, "Synchronised/unsynchronised measurements based novel fault location algorithm for transmission line," *IET Gener., Transmiss. Distrib.*, vol. 12, no. 7, pp. 1493–1500, Apr. 2018.

[4] T. P. S. Bains, T. S. Sidhu, Z. Xu, I. Voloh, and M. R. D. Zadeh, "Impedance-based fault location algorithm for ground faults in series-capacitor-compensated transmission lines," *IEEE Trans. Power Del.*, vol. 33, no. 1, pp. 189–199, Feb. 2018.

[5] Y. Q. Chen, O. Fink, and G. Sansavini, "Combined fault location and classification for power transmission lines fault diagnosis with integrated feature extraction," *IEEE Trans. Ind. Electron.*, vol. 65, no. 1, pp. 561–569, Jan. 2018.

[6] Y. Li, X. Meng, and X. Song, "Application of signal processing and analysis in detecting single line-to-ground (SLG) fault location in high-impedance grounded distribution network," *IET Gener., Transmiss. Distrib.*, vol. 10, no. 2, pp. 382–389, 2016.

[7] K. Sun, Q. Chen, and Z. Gao, "An automatic faulted line section location method for electric power distribution systems based on multisource information," *IEEE Trans. Power Del.*, vol. 31, no. 4, pp. 1542–1551, Aug. 2016.

[8] L. Yuansheng, W. Gang, and L. Haifeng, "Time-domain fault-location method on HVDC transmission lines under unsynchronized two-end measurement and uncertain line parameters," *IEEE Trans. Power Del.*, vol. 30, no. 3, pp. 1031–1038, Jun. 2015.
[9] R. Li, L. Xu, and L. Yao, "DC fault detection and location in meshed multiterminal HVDC systems based on DC reactor voltage change rate," *IEEE Trans. Power Del.*, vol. 32, no. 3, pp. 1516–1526, Jun. 2017.
[10] J. Beerten, S. Cole, and R. Belmans, "Modeling of multi-terminal VSC HVDC systems with distributed DC voltage control," *IEEE Trans. Power Syst.*, vol. 29, no. 1, pp. 34–42, Jan. 2014.
[11] M. Monadi, C. Koch-Ciobotaru, A. Luna, J. I. Candela, and P. Rodriguez, "Multi-terminal medium voltage DC grids fault location and isolation," *IET Gener., Transmiss. Distrib.*, vol. 10, no. 14, pp. 3517–3528, Oct. 2016.
[12] M. Majidi, A. Arabali, and M. Etezadi-Amoli, "Fault location in distribution networks by compressive sensing," *IEEE Trans. Power Del.*, vol. 30, no. 4, pp. 1761–1769, Aug. 2015.
[13] Q. Lin, G. Luo, and J. He, "Travelling-wave-based method for fault location in multi-terminal DC networks," *J. Eng.*, vol. 2017, no. 13, pp. 2314–2318, 2017.
[14] J. Ding, L. Li, Y. Zheng, C. Zhao, H. Chen, and X. Wang, "Distributed travelling-wave-based fault location without time synchronisation and wave velocity error," *IET Gener., Transmiss. Distrib.*, vol. 11, no. 8, pp. 2085–2093, Jun. 2017.
[15] F. V. Lopes, K. M. Dantas, K. M. Silva, and F. B. Costa, "Accurate two-terminal transmission line fault location using traveling waves," *IEEE Trans. Power Del.*, vol. 33, no. 2, pp. 873–880, Apr. 2018.
[16] R. J. Hamidi and H. Livani, "Traveling-wave-based fault-location algorithm for hybrid multiterminal circuits," *IEEE Trans. Power Del.*, vol. 32, no. 1, pp. 135–144, Feb. 2017.
[17] F. V. Lopes, B. F. Kusel, and K. M. Silva, "Traveling wave-based fault location on half-wavelength transmission lines," *IEEE Latin Amer. Trans.*, vol. 14, no. 1, pp. 248–253, Jan. 2016.
[18] P. Wang, B. Chen, H. Zhou, T. Cuihua, and B. Sun, "Fault location in resonant grounded network by adaptive control of neutral-to-earth complex impedance," *IEEE Trans. Power Del.*, vol. 33, no. 2, pp. 689–698, Apr. 2018.
[19] M. Davoudi, J. Sadeh, and E. Kamyab, "Transient-based fault location on three-terminal and tapped transmission lines not requiring line parameters," *IEEE Trans. Power Del.*, vol. 33, no. 1, pp. 179–188, Feb. 2018.
[20] J. Suonan, S. Gao, G. Song, Z. Jiao, and X. Kang, "A novel fault-location method for HVDC transmission lines," *IEEE Trans. Power Del.*, vol. 25, no. 2, pp. 1203–1209, Apr. 2010.
[21] Z.-Y. He, K. Liao, X.-P. Li, S. Lin, J.-W. Yang, and R.-K. Mai, "Natural frequency-based line fault location in HVDC lines," *IEEE Trans. Power Del.*, vol. 29, no. 2, pp. 851–859, Apr. 2014.
[22] M. Fink, "Time reversal of ultrasonic fields—Part I: Basic principles," *IEEE Trans. Ultrason., Ferroelectr., Freq. Control*, vol. 39, no. 5, pp. 555–566, Sep. 1992.
[23] F. Wu, J.-L. Thomas, and M. Fink, "Time reversal of ultrasonic fields—Part II: Experimental results," *IEEE Trans. Ultrason., Ferroelectr., Freq. Control*, vol. 39, no. 5, pp. 567–578, Sep. 1992.
[24] D. Cassereau and M. Fink, "Time-reversal of ultrasonic fields. III. Theory of the closed time-reversal cavity," *IEEE Trans. Ultrason., Ferroelectr., Freq. Control*, vol. 39, no. 5, pp. 579–592, Sep. 1992.
[25] G. Lugrin, N. M. Parra, F. Rachidi, M. Rubinstein, and G. Diendorfer, "On the location of lightning discharges using time reversal of electromagnetic fields," *IEEE Trans. Electromagn. Compat.*, vol. 56, no. 1, pp. 149–158, Feb. 2014.
[26] R. Razzaghi, G. Lugrin, H. M. Manesh, C. Romero, M. Paolone, and F. Rachidi, "An efficient method based on the electromagnetic time reversal to locate faults in power networks," *IEEE Trans. Power Del.*, vol. 28, no. 3, pp. 1663–1673, Jul. 2013.
[27] X. Zhang, N. Tai, Y. Wang, and J. Liu, "EMTR-based fault location for DC line in VSC-MTDC system using high-frequency currents," *IET Gener., Transmiss. Distrib.*, vol. 11, no. 10, pp. 2499–2507, 2017.
[28] R. Razzaghi, G. Lugrin, F. Rachidi, and M. Paolone, "Assessment of the influence of losses on the performance of the electromagnetic time reversal fault location method," *IEEE Trans. Power Del.*, vol. 32, no. 5, pp. 2303–2312, Oct. 2017.
[29] A. Codino, Z. Wang, R. Razzaghi, M. Paolone, and F. Rachidi, "An alternative method for locating faults in transmission line networks based on time reversal," *IEEE Trans. Electromagn. Compat.*, vol. 59, no. 5, pp. 1601–1612, Oct. 2017.

XIPENG ZHANG was born in Jiangsu, China. He is currently pursuing the Ph.D. degree in electrical engineering with Shanghai Jiao Tong University, Shanghai, China. His research interest includes fault location method in power networks, especially in the VSC-HVDC and HVDC transmission lines.

NENGLING TAI (M'07) received the B.Sc., M.Sc., and Ph.D. degrees in electrical engineering from the Huazhong University of Science and Technology (HUST), Wuhan, China, in 1994, 1997, and 2000, respectively. He is currently a Professor with the Department of Power Electrical Engineering, Shanghai Jiao Tong University, Shanghai, China. His research interests include the protection and control of active distribution systems, microgrids, smart grid, and renewable energy.

PAN WU was born in Henan, China. He received the B.Sc. degree in electrical engineering from Shanghai Jiao Tong University, Shanghai, China, in 2013, where he is currently pursuing the Ph.D. degree in electrical engineering. His research interests include topologies, control strategies, and protection schemes for flexible interconnected multiple microgrids.

CHUNJU FAN received the B.S. degree from the Hefei University of Technology, Hefei, China, in 1990, the M.S. degree from Tianjin University, Tianjin, China, in 1993, and the Ph.D. degree from Shanghai Jiao Tong University, Shanghai, in 2005, all in electrical engineering, where she is currently an Associate Professor of electrical engineering. Her research interest includes power system protection.

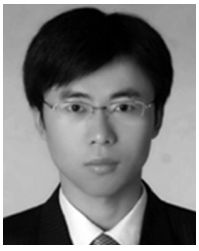

XIAODONG ZHENG (S'12–M'13) was born in Anhui, China, in 1985. He received the Joint Ph.D. degree from the Bradley Department of Electrical and Computer Engineering, Virginia Polytechnic Institute and State University, in 2012, and the Ph.D. degree in electrical engineering from Shanghai Jiao Tong University, Shanghai, China, in 2013. He was a Postdoctoral Researcher with the Department of Electrical and Computer Engineering, Virginia Polytechnic Institute and State University, Blacksburg, VA, USA. He is currently an Associate Professor with the Department of Power Electrical Engineering, Shanghai Jiao Tong University. His research interests include HVDC transmission systems and smart grid.

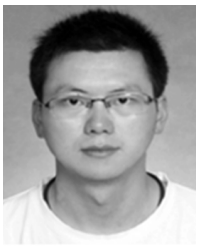

WENTAO HUANG (S'15–M'16) was born in Anhui, China, in 1988. He received the Ph.D. degree in electrical engineering from Shanghai Jiao Tong University, Shanghai, China, in 2015, where he is currently a Lecturer with the Department of Power Electrical Engineering. His research interests include protection and control of active distribution systems, microgrids, smart grid, and renewable energy.